

Comparison of estimated 20-Hz pulse fin whale source levels from the tropical Pacific and Eastern North Atlantic Oceans to other recorded populations

Jennifer L. Miksis-Olds, Danielle V. Harris, and Kevin D. Heaney

Citation: *The Journal of the Acoustical Society of America* **146**, 2373 (2019); doi: 10.1121/1.5126692

View online: <https://doi.org/10.1121/1.5126692>

View Table of Contents: <https://asa.scitation.org/toc/jas/146/4>

Published by the [Acoustical Society of America](https://www.asa.org/)

ARTICLES YOU MAY BE INTERESTED IN

[Ultrasound assessment of translation of microbubbles driven by acoustic radiation force in a channel filled with stationary fluid](#)

The Journal of the Acoustical Society of America **146**, 2335 (2019); <https://doi.org/10.1121/1.5128309>

[Characterizing the seabed in the Straits of Florida by using acoustic noise interferometry and time warping](#)

The Journal of the Acoustical Society of America **146**, 2321 (2019); <https://doi.org/10.1121/1.5127846>

[Multichannel processing of vibrational measurements: A constrained subspace application](#)

The Journal of the Acoustical Society of America **146**, 2350 (2019); <https://doi.org/10.1121/1.5128326>

[A standardized method of classifying pulsed sounds and its application to pulse rate measurement of blue whale southeast Pacific song units](#)

The Journal of the Acoustical Society of America **146**, 2145 (2019); <https://doi.org/10.1121/1.5126710>

[North Atlantic right whale \(*Eubalaena glacialis*\) acoustic behavior on the calving grounds](#)

The Journal of the Acoustical Society of America **146**, EL15 (2019); <https://doi.org/10.1121/1.5115332>

[Acoustic recordings of rough-toothed dolphin \(*Steno bredanensis*\) offshore Eastern Sicily \(Mediterranean Sea\)](#)

The Journal of the Acoustical Society of America **146**, EL286 (2019); <https://doi.org/10.1121/1.5126118>



CAPTURE WHAT'S POSSIBLE
WITH OUR NEW PUBLISHING ACADEMY RESOURCES

Learn more 



Comparison of estimated 20-Hz pulse fin whale source levels from the tropical Pacific and Eastern North Atlantic Oceans to other recorded populations

Jennifer L. Miksis-Olds^{a)}

Center for Acoustics Research and Education, University of New Hampshire, 24 Colovos Road, Durham, New Hampshire 03824, USA

Danielle V. Harris

Centre for Research into Ecological and Environmental Modelling, The Observatory, Buchanan Gardens, University of St. Andrews, Saint Andrews, Fife, KY16 9LZ, United Kingdom

Kevin D. Heaney

Applied Ocean Sciences, 11006 Clara Barton Drive, Fairfax Station, Virginia 22039, USA

(Received 14 June 2019; revised 28 August 2019; accepted 30 August 2019; published online 11 October 2019)

Passive acoustic monitoring, mitigation, animal density estimation, and comprehensive understanding of the impact of sound on marine animals all require accurate information on vocalization source level to be most effective. This study focused on examining the uncertainty related to passive sonar equation terms that ultimately contribute to the variability observed in estimated source levels of fin whale calls. Differences in hardware configuration, signal detection methods, sample size, location, and time were considered in interpreting the variability of estimated fin whale source levels. Data from Wake Island in the Pacific Ocean and off Portugal in the Atlantic Ocean provided the opportunity to generate large datasets of estimated source levels to better understand sources of uncertainty leading to the observed variability with and across years. Average seasonal source levels from the Wake Island dataset ranged from 175 to 188 dB re 1 μ Pa m, while the 2007–2008 seasonal average detected off Portugal was 189 dB re 1 μ Pa m. Owing to the large inherent variability within and across this and other studies that potentially masks true differences between populations, there is no evidence to conclude that the source level of 20-Hz fin whale calls are regionally or population specific.

© 2019 Author(s). All article content, except where otherwise noted, is licensed under a Creative Commons Attribution (CC BY) license (<http://creativecommons.org/licenses/by/4.0/>).

<https://doi.org/10.1121/1.5126692>

[RAD]

Pages: 2373–2384

I. INTRODUCTION

Accurate quantification of marine mammal call source levels is highly sought information because it is essential to determining (1) the range over which marine mammals can effectively communicate and be monitored with passive acoustic technology (McDonald and Fox, 1999), (2) animal density from passive acoustic recordings in certain scenarios (e.g., Küsel *et al.*, 2011; Harris *et al.*, 2018), (3) assessing the potential impacts of sound exposure on marine mammals (Croll *et al.*, 2001; Nowacek *et al.*, 2007; Tyack, 2008), and (4) call function, which is not fully understood in large whales (Charif *et al.*, 2002). Determining the intensity with which mysticete whales produce calls is a major challenge because their large size prohibits measurements in a controlled, captive setting. Consequently, in the absence of direct, empirical measurements, field efforts attempting to estimate source characteristics of large whale vocalizations have utilized a variety of hardware and recording methods ranging from animal-borne acoustic tags (Johnson *et al.*, 2004, 2006; Johnson *et al.*, 2009)

to a large scale Passive Ocean Acoustic Waveguide Remote Sensing (POAWRS) technique (Wang *et al.*, 2016).

Methods employing animal-borne acoustic tags have been largely unsuccessful in acquiring absolute call source levels due to tag placement on the animal. Tags are often attached to the animal behind the sound source, off the acoustic axis of sound production, and in some cases are shadowed by the body making direct and comparable measurements by the tag sensors impossible (Johnson *et al.*, 2009). These obstacles prevent the accurate measurement of highly directional signals like echolocation and greatly complicate measurements of more omni-directional signals like low-frequency baleen whale calls. In limited cases, source parameters have been obtained from vocal recordings of animals in the near vicinity of the tagged animal, but uncertainty was introduced due to parameter estimates because of the unknown distance and orientation between the tagged and nearby vocal animal (Johnson *et al.*, 2006). Work by Goldbogen *et al.* (2014) has more recently demonstrated that high-resolution accelerometry measurements from Digital Acoustic Tags (DTAGs) deployed on a fin whale can distinguish between calls produced by the tagged whale from those produced by conspecifics; this is a current challenge when using tags on baleen whales. Coupling

^{a)}Electronic mail: j.miksisolds@unh.edu

accelerometer measurements to sound pressure measurements on tagged animals will be vital in future tagging studies where identifying the calling animal is required.

Source level estimates of cetaceans from passive acoustic recordings of individual hydrophones, sparse arrays, or array systems all inherently include uncertainty and are generated through a process that relies on assumptions about (sometimes unknown) parameters within the passive sonar equation; hence, it is important to consider all elements of uncertainty, correct for them where possible, or explicitly state any assumptions made when presenting results. With explicitly stated assumptions and best effort in accounting for uncertainty, there is significant value in estimating source levels from the same species and populations with different methods, hardware systems, and under varying propagation conditions. If the estimated source levels are ultimately comparable between methodologies, systems, propagation environments, and assumptions for a single species or population, there is greater confidence in the measurements themselves and the applied products derived from the source levels.

The pulsed 20-Hz whale call of approximately 1 s duration was first attributed to fin whales (*Balaenoptera physalus*) in the western North Atlantic by Schevill *et al.* (1964). The first estimated source level was reported shortly thereafter by Patterson and Hamilton (1964) as a maximum of 180 dB re 1 μ Pa at 1 m. Over the course of decades, estimated source levels were reported for fin whale 20-Hz calls with peak intensity within the 40–15 Hz band in the western

North Atlantic (Watkins *et al.*, 1987), eastern North Pacific (Watkins, 1981; Charif *et al.*, 2002; Weirathmueller *et al.*, 2013), Central/Equatorial Pacific Ocean (Northrop *et al.*, 1968), and Southern Ocean (Širović *et al.*, 2007). The estimated source level range presented by Northrop *et al.* (1968) include calls from Wake Island in the mid-1960s and is a direct geographical comparison to the calls analyzed in this study 50 years later. Table I summarizes estimated source levels of the 20-Hz fin whale call available in the literature for context in digesting the new data from Wake Island and the eastern North Atlantic Ocean populations and for discussing their regional comparability.

The historical summary of fin whale source level estimations in Table I conveys three significant messages. First, each study used different hardware and signal propagation methods in deriving their source level estimates. Second, the sample sizes upon which average source levels were calculated typically numbered in the tens to hundreds of calls. Third, there is a wide range of variability within single studies exceeding 40 dB in some cases. With innovation in recording hardware, sound propagation computing capabilities, and signal processing methods, we have not only been able to greatly increase the sample size of detected calls but also the range over which calls can be detected and subsequently localized (Wang *et al.*, 2016). The goals of this study were to (1) present estimated source levels and (2) understand the factors contributing to the source level estimate variability of the 20-Hz fin whale call from populations in

TABLE I. Summary of fin whale source level (SL) estimates currently available in the scientific literature. All SL values are given in units of dB re 1 μ Pa m. All SL values are assumed to be root-mean-square (rms) values when not explicitly specified in the referenced literature. *Maximum and minimum values obtained from figures contained in the reference. **Personal communication with M. Weirathmueller who performed a re-analysis of the Weirathmueller *et al.* (2013) data using arithmetic averaging. Superscripted numbers indicate geographical locations of each study reflected on the map in Fig. 1.

Location	Authors	Year	System	SL range	SL median	SL mean (using geometric or arithmetic averaging if reported)	Propagation Loss	<i>n</i>
NW Atlantic	Patterson and Hamilton ¹	1964	Bottom mounted and near-surface single and array hydrophones	172–180			Spherical spreading	~500*
NW Atlantic	Watkins <i>et al.</i> ²	1987	Bottom mounted and near-surface single and array hydrophones	160–186			Unspecified	Unspecified
NW Atlantic	Wang <i>et al.</i> ³	2016	Passive Ocean Acoustic Waveguide Remote Sensing (POWARS) towed hydrophone array	166–220* rms	~182* rms	181.9 +/- 5.2 rms	RAM—parabolic equation model	1410
Central Pacific	Northrop <i>et al.</i> ⁴	1968	Water column moored hydrophone array	164–199			Combination of spherical and cylindrical spreading	20
Central Pacific	Harris <i>et al.</i> ⁵	2018	Water column moored hydrophone array	172–185 rms		178 +/- 3 rms (geometric)	Combination of PE modeling and spherical spreading	79
Eastern North Pacific	Charif <i>et al.</i> ⁶	2002	4-hydrophone towed array	159–184	171		Spherical spreading adjusted for Lloyd Mirror effects	34
Eastern North Pacific	Weirathmueller <i>et al.</i> ⁷	2013	OBS	159–200* rms		189.9 +/- 5.8 rms (geometric) 192.1 rms (arithmetic)**	Spherical spreading	1241
Southern Ocean	Širović <i>et al.</i> ⁸	2007	Bottom-moored hydrophone array	180–196		189 +/- 4 (arithmetic)	BELLHOP ray-trace model	83

the eastern North Atlantic and tropical Pacific Oceans. Fin whale calls recorded over a year in the eastern North Atlantic were analyzed from an array of Ocean Bottom Seismometers (OBSs) deployed off the south coast of Portugal. Six years of recordings of fin whale calls in the tropical Pacific Ocean were made off of Wake Island by hydrophones in the Comprehensive Nuclear-Test-Ban Treaty Organization International Monitoring System (CTBTO IMS). Although the recording hardware was different for the two populations, the propagation and application of the signal processing methods used in calculating the estimated source levels were similar with regional modifications. Estimated source levels from this study are then discussed in comparison to other prior published values, methods, and assumptions to assess whether the fin whale 20-Hz call is produced with similar source levels worldwide. See Fig. 1.

II. METHODS

Fin whale source levels were estimated from two different passive acoustic arrays: (1) CTBTO IMS hydrophones at Wake Island in the Pacific Ocean, and (2) OBS array off the coast of Portugal in the NE Atlantic Ocean. Only non-overlapping detections were used in the analyses from both datasets.

A. Source level estimates of fin whale calls from the Wake Island CTBTO station recordings

Fin whale source levels were estimated over a seven-year period from 2007 to 2013 when fin whales recorded on the Wake Island CTBTO IMS hydrophones were seasonally present in tropical waters from November through March (Mizroch *et al.*, 1984; Soule and Wilcock, 2013). Harris *et al.* (2018) presented the estimated source level of 79 fin whale calls from this same northern array dataset that were manually selected and localized over the course of a three-month period from December 2007–February 2008. Harris *et al.* (2018) described the automatic detection, bearing estimation and localization (where possible) of all fin whale calls used in a pilot study estimating fin whale density and distribution using the Wake Island CTBTO IMS sparse array data. In the current study’s methods relating to the CTBTO IMS recordings at Wake Island, automatic detection of fin whale calls, bearing



FIG. 1. (Color online) Recording locations of estimated fin whale source level studies. Numbers are linked to references in Table I. Stars indicate recording locations of the current study off Portugal (NE Atlantic) and Wake Island (Central Pacific).

estimation and localization, and source level estimation parallel those of Harris *et al.* (2018) and will only be summarized here.

The Wake Island station is composed of two three-element triangular arrays with 2 km spacing between elements, with three hydrophones located to the north of the island and three to the south. This study used only data from the northern array where the average water depth was 1425 m (estimated from Amante and Eakins, 2009) and the hydrophones were suspended in the deep sound channel at depths of 731 m (H11N1), 721 m (H11N2), and 746 m (H11N3). Recordings were made continuously at a 250 Hz sampling rate and 24 bit analog-to-digital (A/D) resolution. All three hydrophone channels are digitized underwater at the first connection node using a common reference clock to ensure synchronized recordings. Each hydrophone was calibrated prior to initial deployment in January 2002 and re-calibrated while at-sea in 2011. All hydrophones had a flat (3 dB) frequency response from 8 to 100 Hz, and information from individual hydrophone response curves was applied to the data to obtain absolute values over the full frequency spectrum.

Six full annual migration cycles (November–March) were captured from 2007 to 2013 resulting in approximately 21 600 h of data. Automatic detection of fin whale calls was performed via a spectrogram correlation method applied in the Ishmael bioacoustic analysis software package (Mellinger, 2002). Data were conditioned with a 10–30 Hz bandpass filter prior to cross-correlating the spectrogram time series with a 23–13 Hz, 1-s downsweep synthetic call kernel. Characterization of the automatic detector was achieved by comparing the autodetector results with calls detected manually in a subset of the data. A systematic random subsampling scheme was designed, so that every 155th half-hour segment of data was analyzed manually for fin whale calls. Subsampling in this way ensures a representative sample of the data are analyzed and has been used in other passive acoustic studies (e.g., Marques *et al.*, 2009). With this scheme, a half-hour was analyzed approximately every three days, for a total of 680 analyzed 30-min data segments over the whole study period representing 1.5% of the dataset. This method of subsampling data ensured that a sufficiently large sample of data were manually analyzed (680 samples) and prevented the analyzed data segment from consistently falling on the same day of the week or same time of day, limiting potential bias introduced by consistent anthropogenic noise sources. The optimal detection threshold had a 0.1 false positive proportion and 0.56–0.6 false negative proportion over the 6-year time period. In each segment, calls were manually detected, and the results were compared to the automatic detector results to determine false positive and false negative rates. The detector output fed custom MATLAB (Mathworks, 2016) scripts to determine the root-mean-square (rms) received level and signal-to-noise ratio (SNR) of each detected call. The detector was most efficient at capturing calls with an SNR of 10 dB and higher.

Hyperbolic localization was used to locate fin whale calls and was calculated from the time difference of arrival (TDOA) of a received signal between hydrophone pairs in the three-element array. A simple cross-correlation was first performed to determine time delays; however, environmental heterogeneities caused dispersion in some of the

waveforms traveling from distant ranges rendering the simple cross-correlation a nonviable option for many of the distant calls. If the traditional cross-correlation method failed to produce an acceptable bearing, defined when the three bearings resulting from the three pair combinations all produced bearings within 10 degrees of each other, a band energy analysis was performed. The band energy analysis was conducted on the 10–30 Hz band-pass filtered data and analyzed in 3 Hz bands with 1 Hz overlap, starting at 10 Hz. The peak energy was identified in each band. The first band with a peak of at least 5 dB SNR was selected, and the time index of the first peak in this frequency band for each sensor was used to calculate the time delays. If an acceptable bearing could not be harvested from the band energy analysis, the call was not included in further source level estimates. The median bearing of the cross-correlation or energy band analysis was selected between each pair of hydrophones (N1 and N2, N2 and N3, and N3 and N1). Bearings were rounded to the nearest integer to correspond with the resolution of the propagation model. Location information (range and bearing) and received level was then combined with seasonal propagation loss (Sec. II C) in back calculating the estimated source level using the passive sonar equation.

B. Source level estimates of fin whale calls from the Northeast Atlantic OBS array

The OBS array, deployed between 2007 and 2008, is fully described in [Harris et al. \(2013\)](#). An automatic detector was used to detect fin whale 20-Hz calls using a matched filter run in SEISAN, a seismological software package ([Ottmöller et al., 2011](#)). The matched filter detector used a template call from the OBS dataset with high SNR (specifically a call recorded by OBS10 on 7 January 2008). The vertical OBS channel was used to detect fin whale calls and the data were filtered between 16 and 27 Hz prior to running the detection algorithm. The resulting detections from one of the OBS instruments, OBS19, were processed using SEISAN algorithms to estimate horizontal ranges and relative azimuths to the detected signals following methods described in [Harris et al. \(2013\)](#) and [Matias and Harris \(2015\)](#). Data between 1 December 2007 and 29 February 2008 were used in this study. Further, a smaller sample of manually verified fin whale calls were also analyzed separately. All data were filtered so that the minimum detection threshold was 0.7, the smallest coherency factor between the horizontal and the vertical seismometer channels was 0.1 (full details of the coherency factor are given in [Matias and Harris, 2015](#)) and the minimum SNR was 3.1. These filtering criteria were found to be effective at (a) removing false positives and (b) identifying and removing calls outside the critical range (an important feature of the ranging method; range cannot be estimated beyond the critical range, see [Harris et al., 2013](#) for details). Following filtering using the criteria, the remaining number of detections was 34 321. A false positive analysis of 333 detections throughout the dataset estimated a mean false positive proportion of 0.15 (standard error = 0.03).

The estimated ranges were then adjusted using a ray tracing model, with realistic water and sediment properties (P-wave velocity in the water column = 1.500 km/s, water density = 1.0 g/cm³, P-wave velocity in the sediment = 1.700 km/s, S-wave velocity in the sediment = 0.3 km/s, sediment density = 1.4 g/cm³). A factor of 0.5 was also used to adjust the amplitudes of the horizontal channels to counteract systematic bias observed in the range estimation methodology, thought to be due to the positioning of the OBS just above the seafloor and water column interface ([Matias and Harris, 2015](#)). These values were selected based on work in [Matias and Harris \(2015\)](#). The depth of OBS19 was 4287 m, with a corresponding critical range of 8038 m, assuming the water and sediment velocities above. Finally, calibration data about the orientation of OBS19 was used to convert the estimated relative azimuths to georeferenced absolute azimuths (L. Matias, personal communication).

The propagation loss model used to estimate source levels from the rms received levels on the hydrophone channel was a site- and season-specific parabolic equation, with propagation loss estimated every 5 m (see Sec. II C for more detail). Using the passive sonar equation, source level was estimated using the received level and the propagation loss, $SL = RL + TL$. Although noise was not explicitly accounted for in the equation, only detections with an SNR greater than 10 dB were used in the SL estimates. Using calls with an SNR greater than 10 dB restricts any error caused by integrated noise to be less than 0.5 dB ([Cato, 1998](#)).

Source levels were estimated for all automatic detections. In addition, source levels were estimated for a manually verified sample of 41 calls selected from OBS19 on 3 December 2007 between 0000 and 0100, and were likely produced by the same animal.

C. Propagation loss modeling

The propagation loss (PL) due to range-dependent propagation between a vocalizing whale and receiver using a 17–23 Hz band (1 Hz spacing) was modeled along 360 bearings at 1° resolution using the Peregrine parabolic equation model out to 20 km from H11N1 ([Heaney and Campbell, 2016](#)) and out to 7 km for the OBS array. The propagation loss was modeled using seasonal range-dependent oceanography.¹ It was assumed that the fin whale source was at a depth of 15 m, in keeping with results about fin whale calling behavior ([Stimpert et al., 2015](#)). The bathymetry was taken from the global bathymetry database ETOPO1 ([Amante and Eakins, 2009](#)). Surface loss was negligible due to the low frequency of signals. Sea floor parameters of soft sand sediment were used representing a global average of deep ocean sediment. Details of the geoacoustics parameters in the open ocean (near Wake Island and the OBS array) are not well known but should not affect propagation in this environment due to direct path/sound channel propagation. For the CTBTO data from Wake Island, propagation loss was modeled between the fin whale source near the surface and the H11N1 hydrophone at 731 m depth. Modeling of the OBS19 data was done with the receiver placed on the seafloor.

In order to understand the propagation at the two sites, and shed light on sensitivity of the propagation loss, the PL from the Wake Island HA11N1 receiver was modelled over the November-March migration season. The PL vs depth in the upper panel of Fig. 2 was averaged (magnitude pressure squared) across the frequency band and azimuth. There was very little impact of the seasonal sound speed variability on the PL, consistent with the 20 Hz results of Miksis-Olds *et al.* (2015). For the axial receiver, the propagation to a range of 4 km is direct path showing the Lloyd's mirror interference pattern in depth (the coherent interference created by the direct and surface bounce). At 4 km range, for depths less than 100 m there is an acoustic shadow as the downward refracting warm surface waters refracts the direct path energy below the receiver. From 5 km out in range, the bottom bounce arrival, with low enough grazing angles to reflect, is observed. The tapering of the bottom bounce PL with range is due again to the downward refracting axis to surface sound speed profile.

The lower panel of Fig. 2 shows the difference between the Parabolic Equation (PE) and spherical spreading [$20 \cdot \log_{10}(r)$, where r is range in m] for the upper hundred meters of the water column. Note that range in this computation is slant range and not horizontal distance (as marked along the x axis). At short ranges, there is a 6 dB lower PL for the PE due to the constructive interference of the direct and surface bounce. The PE loss is much greater than spherical (~ 10 dB) in the acoustic shadow at 4500 m. Beyond 5 km, when the bottom bounce is present, there is less PL in the PE than in spherical. The location of the bottom bounce arrival in range is sensitive to the local sediment characteristics. For a hard sediment, there may be no acoustic shadow at 4500 m. The variability of the field with range beyond 12 km is due to local bathymetry effects.

Propagation for a receiver on the seafloor is considerably different. The same pair of plots are generated for the OBS19 seafloor receiver in the eastern Atlantic and are shown in Fig. 3. The range extent of localizations for the

OBS data set was ~ 5 km, so this is the maximum propagation range for these plots. With the receiver on the seafloor, the sound that makes it from the ocean surface is propagating at much higher angles, and there are very few refractive effects with range. This leads to a direct-path/surface reflection Lloyd's mirror pattern for all depths and ranges. The PE/Spherical Spreading loss difference plot in the lower panel highlights this. For fin whale source depths near 15 m, there is a 6 dB reduction in PL due to the constructively adding direct and surface bounce. It is worth noting that for 20 Hz sound, the quarter wavelength distance is 19 m. For a dipole with quarter-wavelength spacing in the vertical, the dominant direction is horizontal. This is an argument for the whales transmitting at 15–20 m, rather than 10 m or less, or 30 to 40 m. For this receiver/source geometry, there is almost no sensitivity to sound speed profile or sediment parameters. There is only a small sensitivity to range (and ranging errors). The primary driver of the PL is the sensitivity to fin whale vocalization depth.

D. Investigating the effect of range and bearing on source level estimates

For both datasets in this study, regression analyses were used to investigate the source level estimates as a function of (a) horizontal range and (b) bearing. All data from the Wake Island dataset was combined into a single dataset and analyzed. Both the OBS automatically detected dataset and the manually selected dataset were analyzed separately. A simple linear regression was fitted to all datasets to investigate the effect of range on estimated source level in the statistical software, R vs 3.5.1 (R Core Team, 2018). Influential data points in each of the three datasets were removed after initial model fitting using Cook's Distance measures.

Generalized Additive Models (GAM, Wood, 2006) were used to model estimated source levels as a function of bearing for both the automatically detected datasets. GAMs using cyclical cubic regression splines were selected to allow

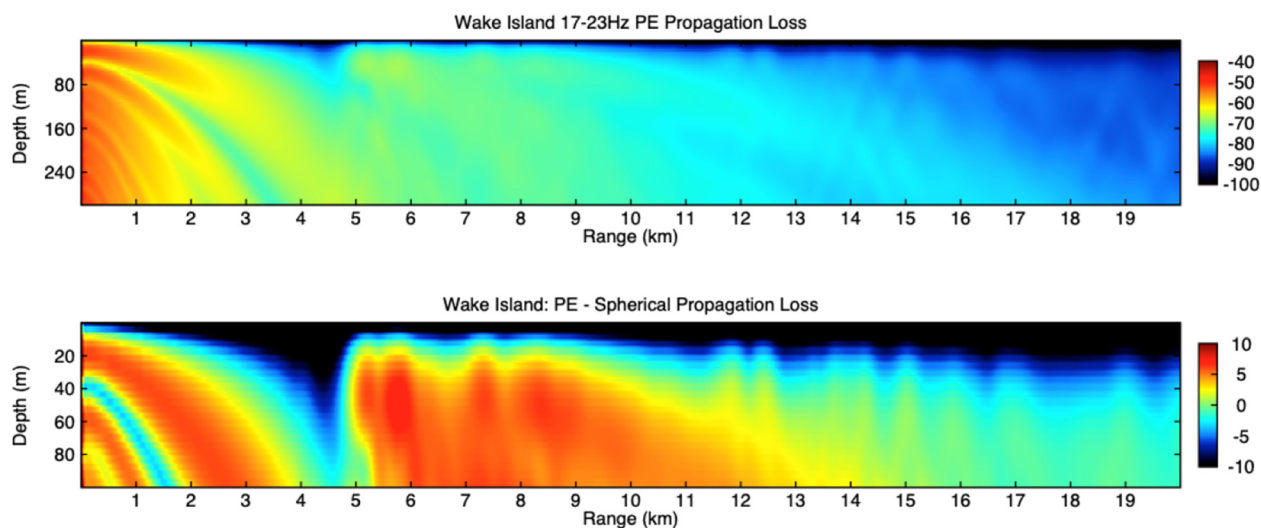


FIG. 2. (Color online) (Top) Parabolic Equation (PE) modeling of propagation loss from the HA11N1 receiver out to 20 km for the upper 300 m of the water column. (Bottom) Difference between Spherical Spreading ($20 \log r$) and the PE propagation loss vs range for the upper 100 m of the water column. Color bars are in dB units.

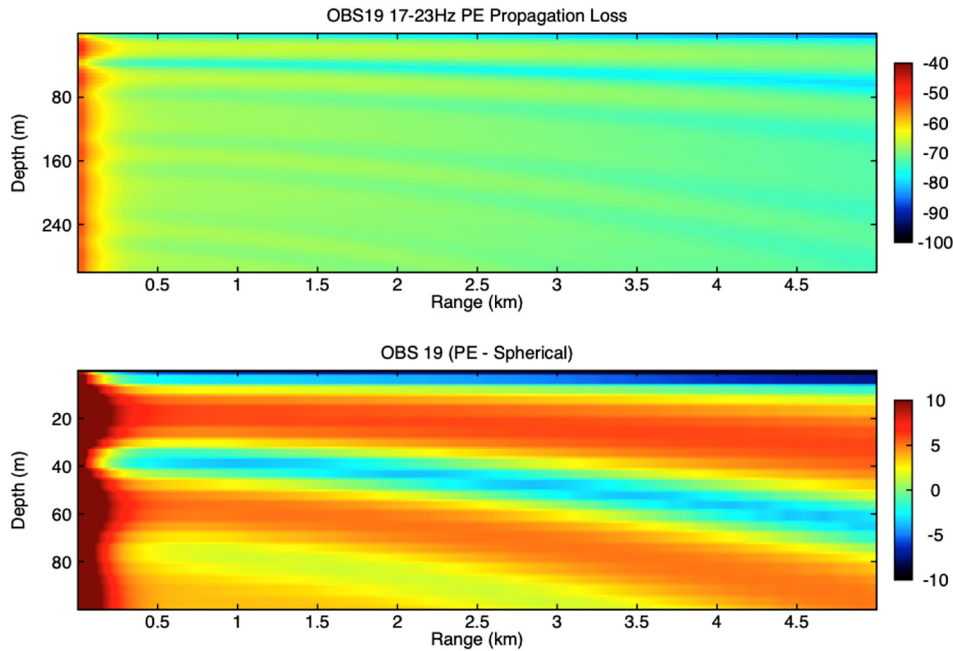


FIG. 3. (Color online) (Top) PE modeling of propagation loss from the OBS19 receiver out to 5 km for the upper 300 m of the water column. (Bottom) Difference between Spherical Spreading ($20 \log r$) and the PE propagation loss vs range for the upper 100 m of the water column. Color bars are in dB units.

a nonlinear, cyclical relationship between estimated source level and bearing; that is, the model accounted for the fact that 359 and 0 degrees are similar values of the predictor variable (bearing in this case). For all fitted models, main model assumptions were checked in R software using diagnostic plots and relevant hypothesis tests.

III. RESULTS

Estimates of fin whale 20-Hz call SL in this study addressed variability in SL related to detection range, propagation loss, detection method, thresholding of autodetections, location, year, and estimated bearing in relation to the receiver. Initial results from the multi-year Wake Island dataset indicated a strong relationship between estimated SL from autodetections and range ($n = 20\,722$), indicating a bias in correctly accounting for PL at greater ranges (Fig. 4). The models did not meet many of the assumptions of linear regression but were designed to take a preliminary look at the pattern between estimated source levels and range, and all models reflected the broad trends seen in the plotted data. The linear regression analyses suggested that fin whale source levels at Wake Island significantly increased as a function of range ($F_{1,19892} = 19\,419$, $p < 0.001$, $R^2 = 0.494$, Fig. 4). When all source level estimates from Wake Island were plotted against range, the linear regression model predicted that source level increased by 3.95 dB/km. When the Wake Island source level estimates were restricted to ranges less than 6 km, the regression predicted an increase of 5.02 dB/km ($F_{1,18639} = 14\,428$, $p < 0.001$, $R^2 = 0.436$, Fig. 6). Further analysis of the Wake Island dataset only included detections less than 6 km, which is consistent with the OBS dataset and ranges detected manually from Wake Island hydrophone data in Harris *et al.* (2018).

To parallel the 79-call manual analysis for estimated fin whale SL from Wake Island in Harris *et al.* (2018), a 41-call manual analysis was conducted for the OBS data to address

potential differences in small sample size, manual analyses (Fig. 5, Table II) and large sample size, automatic detection analyses (Fig. 6, Table II), which are becoming more available with advances in hardware, software, and signal processing methods. The regression model using the automatically detected calls in the OBS dataset predicted a significant but comparatively small increase in source level with range, with an increase of 0.15 dB/km ($F_{1,11194} = 50$, $p < 0.001$, $R^2 = 0.004$, Fig. 6). The regression models for the manually detected OBS dataset predicted that source levels estimated using the PE model did not change significantly as a function of range ($F_{1,36} = 0.001$, $p = 0.97$, $R^2 = 0.000\,035$, Fig. 5). Source levels estimated using spherical spreading were higher than the values estimated using the PE model,

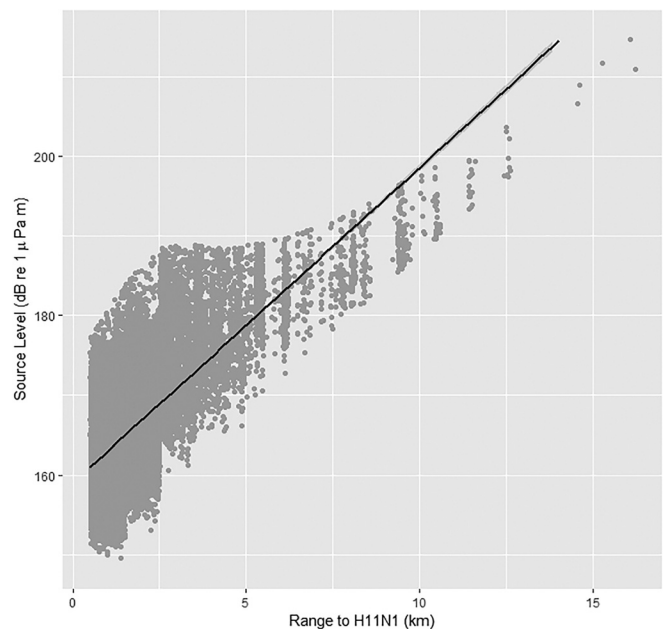


FIG. 4. Estimated fin whale 20 Hz call SL from the Wake Island H11N1 hydrophone ($n = 20\,722$) as a function of range.

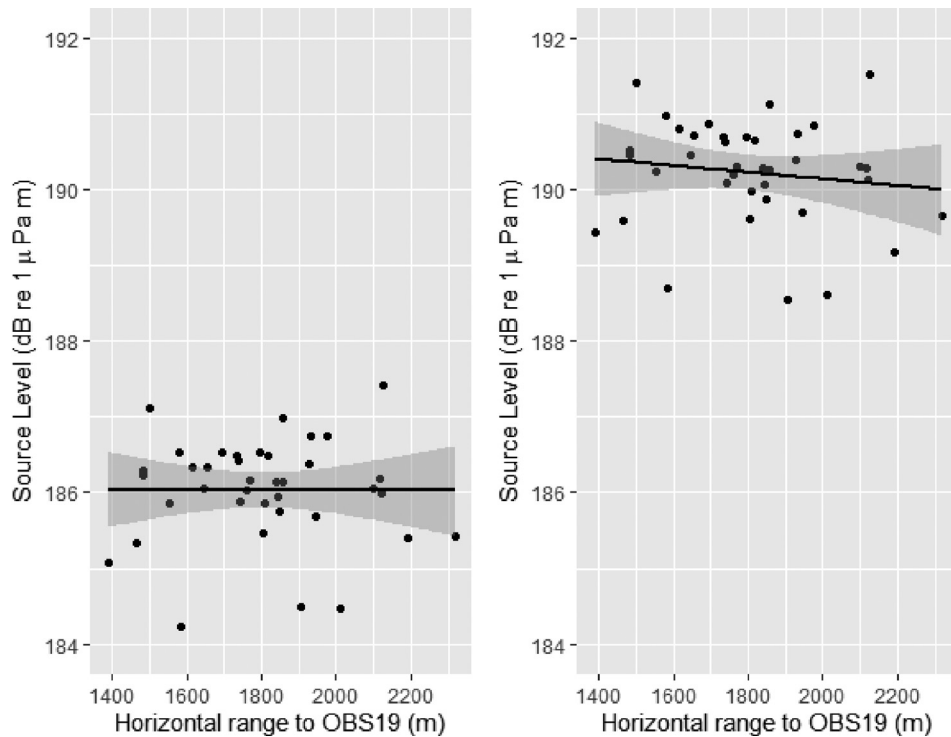


FIG. 5. Manually verified OBS fin whale SL estimates ($n = 41$) calculated using both a PE model (left) and spherical spreading (right) plotted against range. A linear regression line is plotted through each dataset with associated 95% confidence intervals.

but also did not change significantly as a function of horizontal range ($F_{1,36} = 0.699$, $p = 0.41$, $R_2 = 0.02$). Given its more realistic inputs, the PE model was selected as the preferred method of estimating propagation loss in the source level calculations.

Acknowledging the inherent uncertainty and biases related to the propagation loss and autodetectors used in the analysis of the Wake Island data, the multi-year dataset provided the opportunity to explore variability in estimated source levels as a function of year and bearing. The average estimated SL across the six migration seasons did vary from year to year (Table II, Fig. 7), but the differences between and across all years was within the annual median absolute deviation (van der Schaar *et al.*, 2014) (Fig. 7), indicating that the estimated source levels in the Wake Island region were relatively uniform over time.

Estimated SL as a function of bearing was not found to be uniform around the Wake Island H11N1 hydrophone in the Pacific Ocean (Fig. 8). A non-uniform distribution was also

observed around the OBS19 sensor in the Atlantic Ocean (Fig. 8). GAMs (Wood, 2006) were fitted to both automatically detected datasets, with the Wake Island data truncated at 6 km. Both GAMs suggested that source level differed significantly as a function of bearing [Wake Island (WI) model: $F_{6,19493} = 270$, $p < 0.001$, Fig. 8; OBS model: $F_{6,11819} = 97$, $p < 0.001$, Fig. 8]. Both models explained less than 10% of the deviance (WI: 8%; OBS: 5%) suggesting that these models did not adequately capture the variability in the data, but as with the other regression analyses, the models capture the broad pattern observed in the plotted data (Fig. 8).

IV. DISCUSSION

The estimated source levels of the 20-Hz fin whale call obtained in this work in two different oceans overlap with the distributions of all previously published work from the regions of the Southern, Pacific, and Atlantic Oceans (Table I). Estimated source levels from Wake Island recordings in

TABLE II. Estimated fin whale source levels as a function of location, year, sample size, and call detection method. All means are arithmetic unless otherwise specified. Methods for each analyses were consistent across sample size and location within this study and Harris *et al.* (2018)*.

Location	Data duration (months)	Year	Sample Size	Detection Method	PL Model	Estimated mean SL (dB re 1 μ Pa m)
Wake Island, Pacific Ocean	3	2007–2008	79	Manual	PE	178 (geometric)* 179
	5	2007–2008	2238	Auto	PE	184
	5	2008–2009	1267	Auto	PE	178
	5	2009–2010	4268	Auto	PE	178
	5	2010–2011	2759	Auto	PE	175
	5	2011–2012	5187	Auto	PE	180
	5	2012–2013	3876	Auto	PE	188
	30	2007–2013	19 595	Auto	PE	182
Portugal, Atlantic Ocean	3	2007–2008	41	Manual	PE	186
	3	2007–2008	41	Manual	Spherical	190
	3	2007–2008	11 826	Auto	PE	189

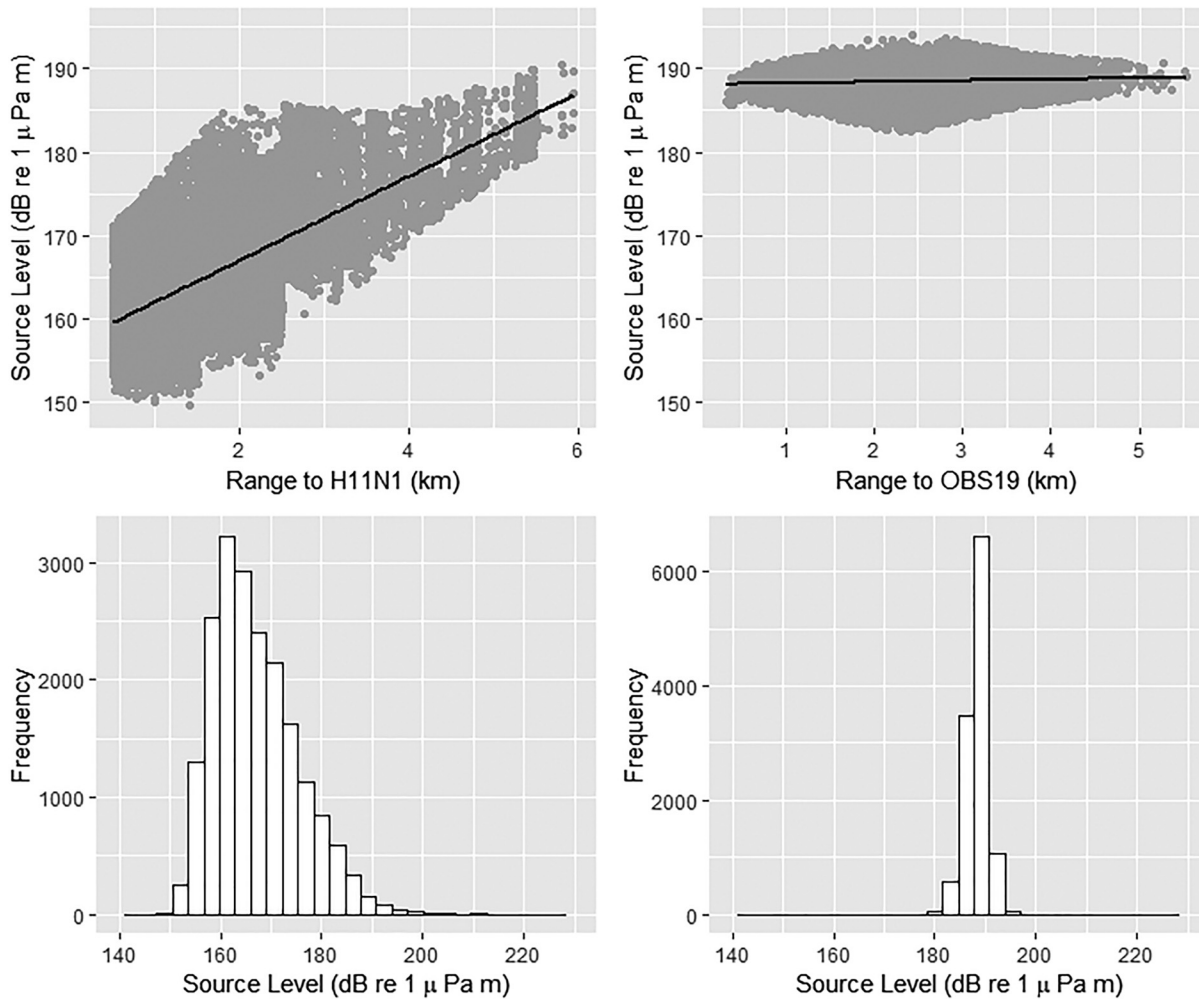


FIG. 6. Estimated fin whale SLs from autodetected signals at Wake Island H11N1 (left, $n = 19\,595$) and OBS19 (right, $n = 11\,826$) plotted against range, with a linear regression line and associated 95% confidence intervals. The confidence intervals are narrow and not clearly visible compared to the data spread on each plot. Bottom histograms reflect the estimated SL distribution at each location.

Northrop *et al.* (1968) and the current study also had almost identical overlap (assuming the differences in data processing were comparable) indicating that the source level of this particular fin whale call did not change drastically over the past 50 years. Given the large range of SL estimates within each study, up to approximately 40 dB in select cases, it is not surprising that global fin whale source level distributions appear rather uniform. However, given the large variabilities in datasets that vary in sample size from tens of samples to tens of thousands of samples in this work, a potentially more informative question to address is whether the mechanism driving the variability observed within a single study is the same mechanism driving variability across different studies.

There is inherent variability in animal source levels that is difficult to adequately capture with only a small number of samples restricted to a small number of detection ranges. The sizeable sample of calls representing a large number of detection ranges with associated call bearings analyzed in the current study provided the opportunity to explore estimated source level variability at a statistical level that has not been possible in previous studies. Potential sources of variability fall into three general categories: behavior, propagation, and false positives in large automatically detected

datasets. Often, it is not possible to tease apart the effects due to each. For example, individual source level variability within a single fin whale calling bout can be highly variable with source levels differing up to 5 dB (Watkins, 1981; Watkins *et al.*, 1987; Weirathmueller *et al.*, 2013; OBS manually verified data, this study). It is unknown whether the variation is due to amplitude modulation by the whale, slight changes in whale orientation impacting consistent directionality, changes in vertical or horizontal movement, uncertainty in the source localization, ephemeral heterogeneities in the water column, or uncertainty in the propagation loss. It is likely a combination of two or more factors.

Variability related solely to sound propagation effects within a single study include heterogeneities in the propagation medium and unaccounted movements of the hydrophone on moorings related to currents that impact the estimated distance between source and receiver. Small errors in the positions of the sensors can cause substantial systematic errors in the calculated arrival angles and ultimate source location, but error related to the movement of the CTBTO hydrophones was estimated to be low (Nichols and Bradley, 2017). Whereas the earliest studies reporting estimated fin whale 20-Hz call source levels did not detail the signal

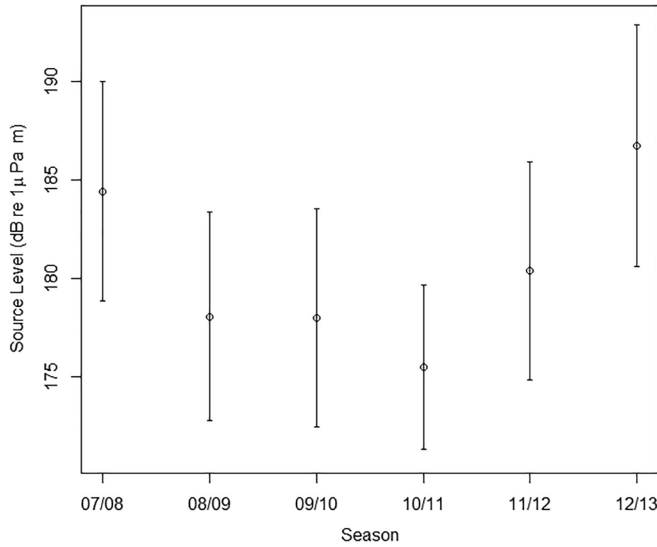


FIG. 7. Annual estimated source level means for detections from Wake Island H11N1. Error bars reflect the median absolute deviation.

processing or propagation loss methods, comparison across more contemporary studies indicate differences in choice of propagation model, assumptions of model input parameters, and signal processing methods. Širović *et al.* (2007) used a hybrid model with a homogeneous sound speed and range independent, flat bottom bathymetry in an upward refracting environment to model propagation loss, while other studies employing a spherical spreading model assumed direct path propagation without consideration for sound speed profile or bathymetry between the source and receiver. Charif *et al.* (2002) used a spherical spreading model and then applied an interference correction factor to account for Lloyd's Mirror Effect that reduced the maximum SL of each call by 6 dB. Alternatively, Wang *et al.* (2016), Harris *et al.* (2018), and this study used a range-dependent parabolic equation model to estimate propagation loss.

Acknowledging that different propagation loss models were employed across studies and may have contributed to variation in estimated source levels, a second source of propagation loss related variability stems from different assumptions in the input parameters of the propagation models. All studies modeled the vocalizing fin whale within the top 60 m of the water column, but the exact source depth differed. Širović *et al.* (2007) modeled the source depth at 30 m, whereas Harris *et al.* (2018) and this work modeled the source depth at 15 m based on tag data from Stimpert *et al.* (2015). Weirathmueller *et al.* (2013) modeled a distribution of vocalizing depths from 5 to 60 m. The actual modeled frequency also differed between studies. For example, Širović *et al.* (2007) modelled a 22 Hz signal, whereas Harris *et al.* (2018) modelled a 20 Hz signal. Environmental noise levels at the time of fin whale call detection were taken into account and detailed in the methods of Weirathmueller *et al.* (2013) and Harris *et al.* (2018), but this passive sonar term was not explicitly addressed in the other studies of Table I. Propagation effects so close to the surface also have the potential to introduce significant levels of variation and uncertainty (Medwin, 2005) to any transmitted signal even if identical propagation loss models, modeled frequency,

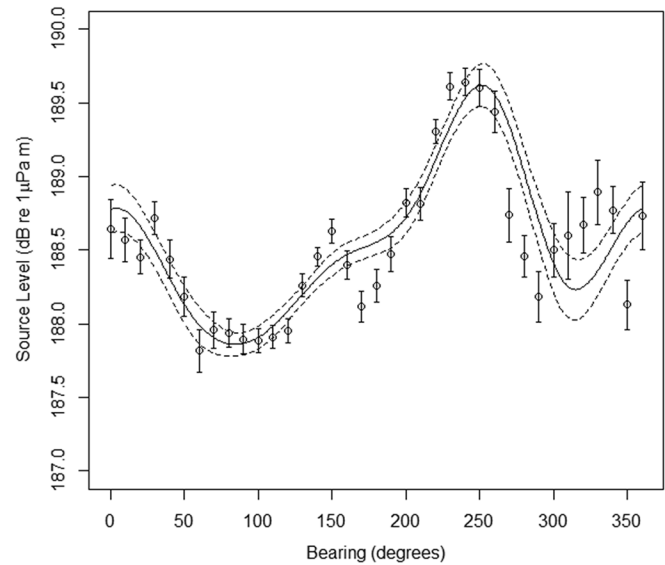
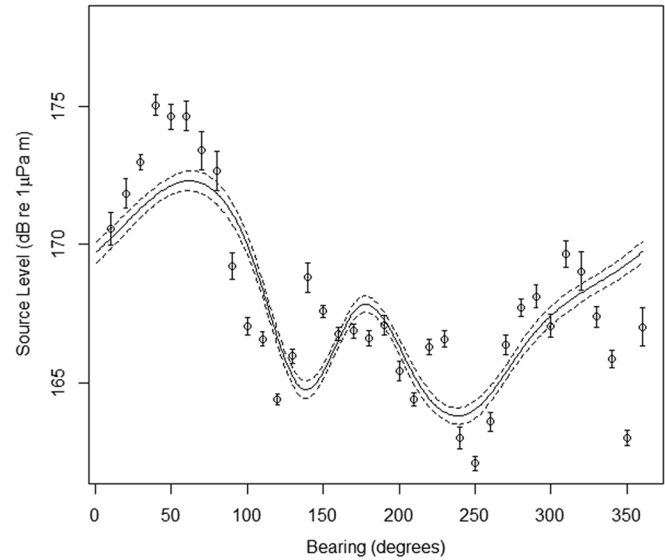


FIG. 8. Estimated source levels from auto detections of Wake Island (top) and OBS (bottom) plotted against bearing, with a smooth GAM overlay.

and input parameters are modeled over time at the same location; it is not surprising to observe a degree of variation across studies in different regions, using different models, and applying different input parameters.

The source and receiver depths, the sound speed profile, the seafloor depth, and source type affect acoustic propagation in the ocean. As illustrated in Figs. 2 and 3, the approximation of propagation loss as spherical $[20 \cdot \log_{10}(\text{Range})]$ is poor. For axial receivers, there are acoustic shadow zones as well as regions of intensification due to bottom bounce energy. For a bottom mounted receiver, the spherical approximation is poor because of the coherent interference between the direct path and the surface reflection. The observation that the estimated source level of fin whales increases significantly with range (in Fig. 6) is likely a signal to noise ratio problem where low source level vocalizations are not detected. For ranges beyond 5 km, the propagation paths include multiple bottom bounces and are influenced by the refraction of the sound speed profile in the upper 10 m of water. A softer sediment in the model

(more lossy) than in reality will reduce the modeled PL with range, requiring an increase in the estimated SL to match the data, as observed. The fall off of PL with range for shallow sources (15 m assumed for fin whales in this study) beyond a distance of 5 km is sensitive to the sound speed field in the upper 100 m, which could have mesoscale ocean structure or surface mixed layers. We have used climatology for the temperature and salinity fields that the sound speed profiles are generated from, and these do not include small scale variability like eddies and surface ducts. The final area of uncertainty in the propagation sensitivity is the source depth. The fall off of PL with range is sensitive to the source depth.

There is also a systematic bias introduced at longer ranges by the detection algorithm. For whales to be detected at longer ranges, in a fixed noise field, they must have positive signal excess. As the range increases and the propagation loss increases, only the loudest transmitted signals can be detected. This will lead to an increase in the median SL as a function of range. This certainly explains the lack of low level whale vocalizations beyond 5 km, but does not explain the observed dramatic rise in the maximum SL with range observed in the Wake Island dataset.

Subtleties of signal processing methods between estimated source level studies are an often overlooked source of bias and variation complicating direct comparisons. The signal duration and bandwidth over which received levels are calculated may or may not be detailed in the study description and have the potential to bias source level estimates. There is the possibility that estimated source levels in [Charif *et al.* \(2002\)](#) that used a 3-s rms window in received level calculations were biased low compared to methods that used either a 1-s window more aligned with the 20-Hz call length ([Širović *et al.*, 2007](#); [Weirathmueller *et al.*, 2013](#)) or manual selection of the call bounds ([Harris *et al.*, 2018](#)). Any thresholding related to signal detection also has the potential to introduce bias to the estimated source level distribution. [Wang *et al.* \(2016\)](#) used a threshold of 10 dB SNR above which detected calls were included in further analysis. The estimated source levels presented in the current study did not have a threshold based on SNR applied for the Wake Island data, though a 10 dB SNR threshold was applied to the OBS dataset consistent with [Wang *et al.* \(2016\)](#). It is unclear and unlikely that the other studies listed in [Table I](#) thresholded based on SNR due to small sample sizes. A last signal processing component to note is the use of broadband equivalent pulse-compression gains applied in [Wang *et al.* \(2016\)](#), which resulted in a 6 dB difference between distributions means depending on whether the gains were applied. The mean estimated source level of the 20-Hz call was 6 dB less when beamforming gains were incorporated in the calculations compared to when no beamforming was applied.

Finally, as datasets become larger, and therefore more reliant on automated detection methods, the influence of false positive detections needs consideration. False positive rates can be estimated (as in this study), which are informative, but the potential bias and uncertainty in source level estimates caused by false detections can only be eliminated if those detections are removed from the dataset. False positives were not removed in the two automated datasets in this

study; exploration of the effect of false detections on these datasets would be a natural extension to this work. However, it is unlikely that false positives are solely responsible for the systematic increase in estimated source level with range as observed in both automated datasets.

All potential sources of uncertainty and bias resulting from propagation model selection, model assumptions, input parameter assumptions, and signal processing differences contributed to a wide variability in the estimated source level distributions both within and across studies and contribute to explaining the greater than 40 dB differences within a single study. However, despite estimated source levels from different time periods, geographical locations, and fin whale populations, it appears that estimated fin whale source level of the 20-Hz call is relatively robust to analysis method, hardware configurations, and environments. At this point, it is not possible to conclusively determine whether fin whale source levels differ across regions, populations, or time periods due to large amount of variability. The work presented here introduces a new dimension to consider in association of interpreting fin whale source levels, namely, call bearings. Detected call bearings estimated over multiple years exhibited a pattern where calls detected along some bearings were consistently louder than those of others. This could be attributed to all the sources of variability, uncertainty, and bias already discussed. In particular, propagation loss differs as a function of direction and therefore estimated source level distributions may vary depending on direction, e.g., if propagation conditions are favorable in one direction, then more calls with lower source levels may be detected, compared to another direction with high propagation loss where only the loudest calls can be detected. This variability in the probability of detecting calls as a function of bearing has not been explicitly corrected for in this study but would be the next step in better understanding the observed patterns. However, an alternative explanation rooted in ecology might also be considered, and is related to behavior and cognition associated with communication.

Is it possible that fin whales are cognizant of their regional landscape to modify source level consistent with bathymetric features? Humans do this naturally when we increase our volume to communicate with someone around a corner and out of sight compared to communicating with someone the same distance away but in a direct line of sight. The Acoustic Adaptation Hypothesis (AAH) predicts that local habitat characteristics influence signal evolution through effects on signal transmission ([Morton, 1975](#)). Consistent with the AAH is the concept that communication signals central to social behavior should be adapted to the local environment to enhance transmission and reception ([Bradbury and Vehrencamp, 2011](#)). The relationship supporting the co-evolution of animal communication and the environment has been illustrated in acoustic communication of fish, birds, frogs, insects, and mammals ([Boncoraglio and Saino, 2007](#); [Ey and Fischer, 2009](#); [Amorim *et al.*, 2018](#)). Specific to amplitude is the Lombard Effect—the involuntary tendency of humans to increase vocal amplitude when speaking in loud noise to enhance the audibility of their transmission ([Lombard, 1911](#))—which has been observed in humans, marine mammals, non-human primates, bats, and

rodents (Hotchkiss and Parks, 2013). There is no named theory or effect to capture amplitude modification in response to the physical structure (bathymetry in this context), but the concept is captured in the sensory drive framework within the AAH theorizing that natural selection will favor signals, behaviors, and receptors that maximize detection and recognition (Endler, 1992). It is unknown whether large whales possess the landscape awareness to modify call amplitude when signaling in different directions, but it is not unreasonable to conjecture that evolution has shaped vocal behavior in whales to cope with this aspect of their environment.

A. Implications for SL in density estimation

It is clear from the review of fin whale source level estimates in this study that estimates may vary due to differences in the methods used for estimation. Due to the multiple steps involved in source level estimation, it is not always easy to assess where bias and imprecision may be introduced. However, it is possible to investigate the impact that biased source level estimates could have on density estimation methods that rely on such inputs. Here, the pilot study analysis presented in Harris *et al.* (2018) was re-analyzed, except that the source level distribution was altered to reflect a 6 dB bias in either direction. The assumed source level distribution used in the original study had a geometric mean of 177.7 dB re 1 μ Pa m (standard deviation: 3.30, $n = 79$). The original study estimated that an area of up to 973 km² was monitored, leading to an initial density estimate of 0.32 animals/1000 km² [coefficient of variation (CV): 0.52]. By increasing the assumed source level to 183.7 dB re 1 μ Pa m (with the same standard deviation), the estimated monitored area increased to 4575 km² with an associated density estimate of 0.07 animals/1000 km² (CV: 0.52). Conversely, assuming a lower source level of 171.7 dB re 1 μ Pa m resulted in a reduced estimated monitored area of 236 km² and a density estimate of 1.3 animals/1000 km² (CV: 0.52). Therefore, it is clear that bias in source level estimation has the potential to alter density estimates, and associated monitored area sizes, by an order of magnitude when using density estimation methods that rely on source level inputs.

V. CONCLUSIONS

Direct source level measurements of large whale vocalizations are extremely difficult to make, yet accurate source level information is incredibly important in applications related to monitoring, passive acoustic density estimation, and effective communication. Recognizing the need and value of call source level for numerous applications, multiple studies have estimated the source level of the fin whale 20-Hz call over time and geographical region. This study provided a unique opportunity to assess estimates of fin whale source level within the context of previous work to evaluate regional specificity or global uniformity in population source levels, to measure source levels over time, to measure source level as a function of bearing in relation to the recorder, and to identify factors contributing to the source level estimate variability of the 20-Hz fin whale call from populations in the eastern Northeast Atlantic and tropical Pacific Oceans. Results indicate that variability related to back

calculations of source level from received levels via the passive sonar equation stems largely from uncertainty in the propagation loss term with additional variability introduced by methods related to data collection and signal detection. Acknowledging these uncertainties, it appears that estimates of the 20-Hz fin whale call are relatively robust to hardware configuration, method of estimating propagation loss, sample size, detection method, time, and space; owing to the large inherent variability within and across this and other studies that potentially masks any true difference between populations, there is no evidence at this time to conclude that the source level of 20-Hz fin whale calls are regionally or population specific.

ACKNOWLEDGMENTS

D.H. was funded by the Office of Naval Research (Award: N00014-16-1-2364). J.M.O. was funded under Award: N00014-16-1-2860 also from the Office of Naval Research. The CTBTO data were accessed from the Air Force Tactical Applications Center/US National Data Center. Thanks are extended to James Neely (AFTAC), Richard Baumstark (AFTAC), Mark Prior (formerly CTBTO), and Andrew Forbes (formerly CTBTO), Mario Zampolli (CTBTO), Peter Nielsen (CTBTO), and Georgios Haralabus (CTBTO) for their assistance in data transfer and transfer of knowledge of CTBTO data. Thanks also to AFTAC and CTBTO for making the data available (CTBTO Virtual Data Exploitation Centre (vDEC): <https://www.ctbto.org/specials/vdec/>). Please note that the views expressed in this study are those of the authors and do not necessarily represent the views of the CTBTO Preparatory Commission. The Gulf of Cadiz data were collected for the NEAREST project, on behalf of the EU Specific Programme “Integrating and Strengthening the European Research Area,” Sub-Priority 1.1.6.3, “Global Change and Ecosystems,” Contract No. 037110. The authors thank Professor Luis Matias and Dr. Andreia Pereira at the Instituto Dom Luiz, Universidade de Lisboa for access to the NEAREST data and assistance during the data analysis.

¹Temperature and salinity fields from the World Ocean Atlas can be found at <https://www.nodc.noaa.gov/OC5/indprod.html>

- Amante, C., and Eakins, B. W. (2009). “ETOPO1 1 Arc-Minute Global Relief Model: Procedures, Data Sources and Analysis,” NOAA Technical Memorandum NESDIS NGDC-24. National Geophysical Data Center, NOAA, Silver Spring, MD.
- Amorim, M. C. P., Vasconcelos, R. O., Bolgan, M., Pedroso, S. S., and Fonseca, P. J. (2018). “Acoustic communication in marine shallow waters: Testing the acoustic adaptive hypothesis in sand gobies,” *J. Exp. Biol.* **221**(22), 183681.
- Boncoraglio, G., and Saino, N. (2007). “Habitat structure and the evolution of bird song: A meta-analysis of the evidence for the acoustic adaptation hypothesis,” *Funct. Ecol.* **21**, 134–142.
- Bradbury, J. W., and Vehrencamp, S. L. (2011). *Principles of Animal Communication*, 2nd ed. (Sinauer Associates, Sunderland, MA).
- Cato, D. H. (1998). “Simple methods of estimating source levels and locations of marine animal sounds,” *J. Acoust. Soc. Am.* **104**(3), 1667–1678.
- Charif, R. A., Mellinger, D. K., Dunsmore, K. J., Fristrup, K. M., and Clark, C. W. (2002). “Estimated source levels of fin whale (*Baleoptera physalus*) vocalisations: Adjustments for surface interference,” *Mar. Mam. Sci.* **18**, 81–98.

- Croll, D. A., Clark, C. W., Calambokidis, J., Ellison, W. T., and Tershy, B. (2001). "Effect of anthropogenic low-frequency noise on the foraging ecology of Balaenoptera whales," *Animal Conserv.* **4**, 13–27.
- Ender, J. A. (1992). "Signals, signal conditions, and the direction of evolution," *Am. Nat.* **139**, S125–S153.
- Ey, E., and Fischer, J. (2009). "The 'acoustic adaptation hypothesis'—A review of the evidence from birds, anurans and mammals," *Bioacoustics* **19**, 21–48.
- Goldbogen, J. A., Stimpert, A. K., DeRuiter, S. L., Calambokidis, J., Friedlaender, A. S., Schorr, G. S., Moretti, D. J., Tyack, P. L., and Southall, B. L. (2014). "Using accelerometers to determine the calling behavior of tagged baleen whales," *J. Exp. Biol.* **217**, 2449–2455.
- Harris, D., Matias, L., Thomas, L., Harwood, J., and Geissler, W. (2013). "Applying distance sampling to fin whale calls recorded by single seismic instruments in the northeast Atlantic," *J. Acoust. Soc. Am.* **134**, 3522–3535.
- Harris, D. V., Miksis-Olds, J. L., Vernon, J. A., and Thomas, L. (2018). "Fin whale density and distribution estimation using acoustic bearings derived from sparse arrays," *J. Acoust. Soc. Am.* **143**(5), 2980–2993.
- Heaney, K. D., and Campbell, R. L. (2016). "Three-dimensional parabolic equation modeling of mesoscale eddy deflection," *J. Acoust. Soc. Am.* **139**, 918–926.
- Hotchkin, C., and Parks, S. (2013). "The Lombard effect and other noise-induced vocal modifications: Insight from mammalian communication systems," *Biol. Rev.* **88**(4), 809–824.
- Johnson, M., de Soto, N. A., and Madsen, P. T. (2009). "Studying the behaviour and sensory ecology of marine mammals using acoustic recording tags: A review," *Mar. Ecol. Prog. Ser.* **395**, 55–73.
- Johnson, M., Madsen, P. T., Zimmer, W. M. X., De Soto, N. A., and Tyack, P. L. (2004). "Beaked whales echolocate on prey," *Proc. R. Soc. Lond. B* **271**(Suppl 6), S383–S386.
- Johnson, M., Madsen, P. T., Zimmer, W. M. X., De Soto, N. A., and Tyack, P. L. (2006). "Foraging Blainville's beaked whales (*Mesoplodon densirostris*) produce distinct click types matched to different phases of echolocation," *J. Exp. Biol.* **209**(24), 5038–5050.
- Küsel, E. T., Mellinger, D. K., Thomas, L., Marques, T. A., Moretti, D. J., and Ward, J. (2011). "Cetacean population density from single fixed sensors using passive acoustics," *J. Acoust. Soc. Am.* **129**, 3610–3622.
- Lombard, E. (1911). "Le signe de l'elevation de la voix" ("The sign of the elevation of the voice"), *Annales des Maladies de l'Oreille et du Larynx* **37**, 101–119.
- Marques, T. A., Thomas, L., Ward, J., DiMarzio, N., and Tyack, P. L. (2009). "Estimating cetacean population density using fixed passive acoustic sensors: An example with Blainville's beaked whales," *J. Acoust. Soc. Am.* **125**, 1982–1994.
- MathWorks (2016). MATLAB documentation.
- Matias, L., and Harris, D. (2015). "A single-station method for the detection, classification and location of fin whale calls using ocean-bottom seismic stations," *J. Acoust. Soc. Am.* **138**(1), 504–520.
- McDonald, M. A., and Fox, C. G. (1999). "Passive acoustic methods applied to fin whale population density estimation," *J. Acoust. Soc. Am.* **105**(5), 2643–2651.
- Medwin, H. (2005). *Sounds in the Sea: From Ocean Acoustics to Acoustical Oceanography* (Cambridge University Press, Cambridge, UK).
- Mellinger, D. K. (2002). "Ishmael 1.0 User's Guide," NOAA Technical Memorandum OAR PMEL-120, NOAA/PMEL, Seattle, WA.
- Miksis-Olds, J. L., Vernon, J. A., and Heaney, K. D. (2015). "The impact of ocean sound dynamics on estimates of signal detection range," *Aquatic Mammals (Special ESOMM Edition)* **41**, 444–454.
- Mizroch, S. A., Rice, D. W., and Breiwick, J. M. (1984). "The fin whale, *Balaenoptera physalus*," *Mar. Fish. Rev.* **46**, 20–24.
- Morton, E. S. (1975). "Ecological sources of selection on avian sounds," *Am. Nat.* **109**, 17–34.
- Nichols, S. M., and Bradley, D. L. (2017). "In situ shape estimation of triangular moored hydrophone arrays using ambient signals," *IEEE J. Oceanic Eng.* **42**(4), 923–935.
- Northrop, J., Cummings, W., and Thompson, P. (1968). "20-Hz signals observed in the central Pacific," *J. Acoust. Soc. Am.* **43**, 383–384.
- Nowacek, D., Thorne, L., Johnston, D., and Tyack, P. (2007). "Responses of cetaceans to anthropogenic noise," *Mam. Rev.* **37**, 81–115.
- Ottmøller, L., Voss, P., and Havskov, J. (2011). "Seisan earthquake analysis software for Windows, Solaris, Linux and MacOSX," in *Department of Earth Sciences, University of Bergen, Bergen, Norway*, p. 335.
- Patterson, B., and Hamilton, G. (1964). "Repetitive 20 cycle per second biological hydroacoustic signals at Bermuda," in *Marine Bio-Acoustics*, edited by W. Tavolga (Pergamon Press, New York), pp. 125–145.
- R Core Team (2018). R: A language and environment for statistical computing; 2015.
- Schevill, W. E., Watkins, W. A., and Backus, R. H. (1964). "The 20-cycle signals and Balaenoptera (fin whales)," in *Marine Bio-Acoustics*, edited by W. N. Tavolga (Pergamon, Oxford, UK), pp. 147–152.
- Širović, A., Hildebrand, J. A., and Wiggins, S. M. (2007). "Blue and fin whale call source levels and propagation range in the Southern Ocean," *J. Acoust. Soc. Am.* **122**, 1208–1215.
- Soule, D. C., and Wilcock, W. S. (2013). "Fin whale tracks recorded by a seismic network on the Juan de Fuca Ridge, Northeast Pacific Ocean," *J. Acoust. Soc. Am.* **133**(3), 1751–1761.
- Stimpert, A. K., DeRuiter, S. L., Falcone, E. A., Joseph, J., Douglas, A. B., Moretti, D. J., Friedlaender, A. S., Calambokidis, J., Gailey, G., Tyack, P. L., and Goldbogen, J. A. (2015). "Sound production and associated behavior of tagged fin whales (*Balaenoptera physalus*) in the Southern California Bight," *Animal Biotel.* **3**, 23.
- Tyack, P. L. (2008). "Implications for marine mammals of large-scale changes in the marine acoustic environment," *J. Mamm.* **89**(3), 549–558.
- van der Schaar, M., Ainslie, M. A., Robinson, S. P., Prior, M. K., and André, M. (2014). "Changes in 63 Hz third-octave band sound levels over 42 months recorded at four deep-ocean observatories," *J. Mar. Syst.* **130**, 4–11.
- Wang, D., Huang, W., Garcia, H., and Ratilal, P. (2016). "Vocalization source level distributions and pulse compression gains of diverse baleen whale species in the Gulf of Maine," *Remote Sens.* **8**(11), 881.
- Watkins, W. A. (1981). "Activities and underwater sounds of fin whales," *Sci. Rep. Whales Res. Inst.* **33**, 83–117.
- Watkins, W. A., Tyack, P., Moore, K. E., and Bird, J. E. (1987). "The 20-Hz signals of finback whales (*Balaenoptera physalus*)," *J. Acoust. Soc. Am.* **82**, 1901–1912.
- Weirathmueller, M. J., Wilcock, W. S., and Soule, D. C. (2013). "Source levels of fin whale 20 Hz pulses measured in the Northeast Pacific Ocean," *J. Acoust. Soc. Am.* **133**(2), 741–749.
- Wood, S. N. (2006). *Generalised Additive Models: An Introduction with R* (Chapman & Hall, Boca Raton, FL).